Full-Wave Characterization of the Mode Conversion in a Coplanar Waveguide Right-Angled Bend

Ming-Dong Wu, Sheng-Ming Deng, Ruey-Beei Wu, and Powen Hsu

Abstract—**A full-wave algorithm is proposed to analyze thoroughly a 90° bend of coplanar waveguide (CPW). Based on the mixed potential integral equation (MPIE) formulation, the equivalent magnetic current distribution on the apertures is solved by the moment method using overlapping rooftop basis functions and the Galerkin weighting procedure. The matrix pencil approach is then utilized to do the de-embedding procedure and extract both the coplanar and slotline modes scattering off the asymmetric discontinuity. Experiments are performed to measure the scattering parameters and the results verify the accuracy of the present algorithm. The full 4×4 scattering matrix between these two modes is presented and from which, the occurrence of the mode conversion is investigated. The mode conversion is noticed to become almost complete at certain frequencies, which may be useful in the design of CPW to coupled slotline transition.**

I. Introduction

COPLANAR WAVEGUIDE (CPW) has found increasing applications in MIC and MMIC due to several advantages it offers over the conventional microstrip line [1], [2]. These include the ease in connecting shunt lumped elements without using via holes, and the low dispersions of both the propagation constant and the characteristic impedance for the coplanar (even) mode. Also, the propagation constant and the characteristic impedance of CPW can be adjusted by changing the slot width to strip width ratio. There is no need to build an extremely thin, and thus fragile, substrate in the structure miniaturization. However, one of the main obstacles facing CPW is the excitation of the slotline (odd) mode in asymmetric discontinuities, like bends and T-junctions, which are unavoidable in modern circuits where packing density increases with the complexity of the designs [3]. Two remedies have been proposed to suppress the odd mode: one is the use of the air-bridges [4], and the other is the use of the top and/or bottom ground plane shields [5].

During the past few years, several methods have been presented to characterize, theoretically and/or experimentally, CPW asymmetric discontinuities with or without air bridges [6]–[12]. The hybrid technique has been employed to investigate the suppressing effects of the air bridges on shunt stubs [6], [11], [12], bends, and T-junctions [7]. In this technique, the structures without air bridges are first analyzed, and the frequency dependent equivalent circuits are modified by incorporating the air bridge's effect evaluated using a quasi-static model [13]. The finite difference time domain (FDTD) method was implemented to the solutions of band reject filters with and without air bridges and modified T-junctions [8]. A more detailed frequency domain analysis of the same filters was carried out by Omar and Chow [9] using the mixed potential integral equation (MPIE) formulation. Also, the spectral domain method was applied to analyze T-junctions with various types of air bridges [10].

While extensive studies aimed at the suppression of the odd mode, the mode conversion phenomenon itself is comparatively unexploited. In [10], the odd mode excited by the T-junction was obtained by evaluating the inner product between the solved field distributions and the precomputed modal fields. The approach requires the solution of the field in a whole plane transverse to the CPW section and the modal field distribution obtained in the line eigenvalue problem is prerequisite. A better approach is thus proposed in [12], either using Prony's method or the standing-wave method, to extract all the modes scattering off the shunt stub discontinuity. It does not require the modal propagation constants and field distributions, except that the total number of the guided modes must be accurately determined a priori.

In this paper, a full-wave algorithm is proposed to analyze a CPW 90° bend, and a full 4×4 scattering matrix is derived to characterize the mode conversion between the even and odd modes. Based on the MPIE formulation, [14], the algorithm first solves the field problem by the moment method [15] using finite element rooftop basis functions. Given the magnetic current distribution on the apertures, the matrix pencil approach [16] is then employed to do the de-embedding procedure and extract the scattering parameters of these two modes. The formulation and theoretical aspects are presented in Section II. This algorithm has the advantage of performing the solution in the space domain directly, which keeps a good physical insight of the problem [17]. Moreover, the parameter extraction involves only the fields on the apertures while the number of guided modes and the propagation constant and modal amplitude of each mode are obtained in posteriori.

The experimental setup is described in Section III. Since the test fixtures are simply terminated with SMA connectors, it is impossible to measure the full 4×4 scattering matrix directly. By assuming that the connectors are almost short circuits for the odd mode, the scattering parameters for the even mode can be derived from the 4×4 scattering matrix and compared with the measured data. In Section IV, numerical results of the full

Manuscript received July 5, 1994; revised August 1, 1995. This work was supported by the National Science Council, Republic of China, Contract NSC84-2221-E002-016.

The authors are with the Department of Electrical Engineering, National Taiwan University, Taipei, Taiwan 10617, Republic of China.

IEEE Log Number 9414855.

4×4 scattering matrix are presented to depict the occurrence of the mode conversion due to the bend discontinuity. Finally, brief conclusions are drawn in Section V.

II. Theory

A. Mixed Potential Integral Equation Formulation

Fig. 1 shows a CPW 90° bend discontinuity in the open region where the ground plane and the dielectric substrate extend to infinity in the x and y directions. The conductor is assumed to be perfect and of zero thickness. The whole region of the original problem can be split into two separate ones by applying the Schekunoff's equivalence principle, which introduces an equivalent magnetic current on the apertures $\mathbf{M}_s$. This magnetic current generates electromagnetic field in the two regions above and below the aperture plane, which can be expressed in terms of mixed vector and scalar potentials. The continuity condition of the tangential magnetic field across the aperture leads to the integral equation [18]

$$\mathbf{e}_z \times \left[\int\int_{S'} j\omega G_F(|\mathbf{r}-\mathbf{r}'|)\mathbf{M}_s(\mathbf{r}')dS' + \int\int_{S'} \nabla G_\Phi(|\mathbf{r}-\mathbf{r}'|)\rho_m(\mathbf{r}')dS' \right] = \mathbf{J}_s(\mathbf{r}) \tag{1}$$

where $\mathbf{J_s}$ is the excitation current, ρ_m is the magnetic charge relating to the magnetic current through the continuity equation

$$\nabla_s' \cdot \mathbf{M}_s(\mathbf{r}') + j\omega\rho_m(\mathbf{r}') = 0 \tag{2}$$

in which ∇_s' denotes taking divergence along the aperture surface at the source point $\mathbf{r}'$, and the vector and the scalar potentials in the aperture plane can be expressed as [18]

$$G_F(r) = \frac{\epsilon_0}{2\pi}\left[\frac{e^{-jk_0 r}}{r} + \epsilon_r \times \int_0^\infty J_0(\lambda r)\frac{u+\epsilon_r u_0 \tanh(uh)}{u\cdot \mathrm{DTM}}\lambda d\lambda\right] \tag{3}$$

$$G_\Phi(r) = \frac{1}{2\pi\mu_0}\left\{\frac{e^{-jk_0 r}}{r} + \int_0^\infty J_0(\lambda r)\left[\left(\frac{\epsilon_r k_0^2}{\lambda^2}\frac{u+u_0\epsilon_r\tanh(uh)}{u\cdot\mathrm{DTM}}\right) + \left(\frac{u}{\lambda^2}\frac{u+u_0\coth(uh)}{\mathrm{DTE}}\right)\right]\lambda d\lambda\right\} \tag{4}$$

where

$$\mathrm{DTM} = u_0\epsilon_r + u\tanh(uh)$$
$$\mathrm{DTE} = u_0 + u\coth(uh)$$
$$u_0 = \sqrt{\lambda^2 - k_0^2}$$
$$u = \sqrt{\lambda^2 - \epsilon_r k_0^2}$$

and J_0 is the Bessel function. It should be noted that the integrands of the Sommerfeld integrals in (3) and (4) have some pole singularities and decay very slowly. Special treatment should be employed for a successful numerical evaluation of the integrals [17].

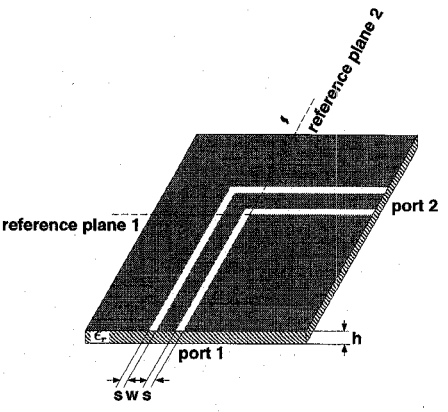

Fig. 1. Schematic view on a coplanar waveguide 90°bend discontinuity.

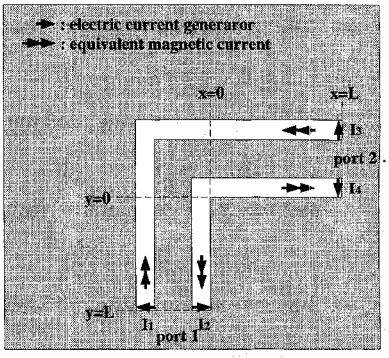

Fig. 2. The finite structure considered in nunerical analysis and the current generators at feeding points.

The equivalent magnetic current on the apertures can be solved from (1) by applying the moment method. The two semi-infinitely long CPW transmission lines are first truncated into finite sections of length L as shown in Fig. 2. Ideal current sources I_1 and I_2 are impressed at the two truncated ends of port 1, while I_3 and I_4 at port 2. The aperture region in the resultant finite bend structure is then divided into a finite number of rectangular cells. As shown in Fig. 3, the unknown magnetic currents, x- and y- directed, are expanded as a finite sum of overlapping rooftop functions

$$\mathbf{M}_s(\mathbf{r}') = \sum_{i=1}^{N} v_i\Lambda_i = \sum_{i=1}^{N} v_i\Lambda_{it}\mathbf{e}_t\ ; \qquad t = x \text{ or } y \tag{5}$$

and the magnetic charges by

$$j\omega\rho_m = \sum_{i=1}^{N} v_i\Pi_i; \qquad \Pi_i = -\nabla_s{}' \cdot \Lambda_i. \tag{6}$$

Note that nonuniform grid division is employed near the discontinuity region to achieve good accuracy while keeping affordable computation load. Since not only the even mode but also the odd mode will be scattered off the bend discontinuity, the coefficients v_i's on the two slots of a CPW can not be assumed of same magnitude and opposite phase.

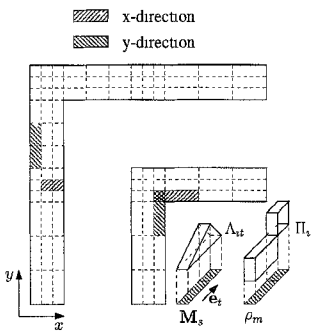

Fig. 3. The cell division and basis functions of equivalent magnetic currents and charges in the moment method analysis.

Substitution of (5) and (6) in (1) with the employment of the Galerkin's weighting procedure yields a system of simultaneous equations

$$\overline{\overline{Y}}\mathbf{V} = \mathbf{I} \tag{7}$$

where $\overline{\overline{Y}}$ is the admittance matrix, $\mathbf{V}$ is a vector of unknown coefficients v_i's, and $\mathbf{I}$ is a vector of given excitation currents. Since the scattering matrix of the discontinuity is, by definition, independent of the feeding and termination, the excitation currents here, for simplicity, are choosen to be zero everywhere except at the feeding points. Also, the structure in Fig. 2 is finite and no sort of absorbing boundary conditions need be enforced at the truncated end.

B. Extraction of Scattering Matrix

The magnetic current along the CPW section can be described by the superposition of the even and odd modes and other higher order modes, each one having its own spatial parameters [12]. For example, consider the section of port 2 from $x = 0$ to L in Fig. 2, where a uniform mesh division of constant interval s in x-direction is chosen in moment method solution. Given the solved coefficients v_i's, one can find the total longitudinal magnetic current at each sampled point along the two slot sections. Physically, it is the line voltage from the center strip to the ground across a particular slot. Let $v_{e,k}$ denote the voltage of CPW (or even) mode at the k'th sampled point, which is determined from average of the line voltages across the two slots. Then $v_{e,k}$ can be written as

$$v_{e,k} \cong \sum_{i=1}^{n} c_i \, \mathrm{e}^{\gamma_i k s}; \quad k = 0, 1, 2, \ldots, N_T - 1 \tag{8}$$

where N_T is the number of the sampled points, n is the number of significant modes (the incoming and outgoing modes treated as two different ones), γ_i is the complex propagation constant of the i'th mode, and c_i is the modal voltage.

Equation (8) is a typical problem of extracting poles from a sampled system response. The matrix pencil method can be employed to successfully solve the problem [16], [19]. The solution procedure is briefly summaried as follows. To begin with, two information matrices $[Y_0]$ and $[Y_1]$ are constructed with element values defined by

$$Y_0(i,j) = v_{e,i+j-2}; \qquad Y_1(i,j) = v_{e,i+j-1} \tag{9}$$

for $i, j = 1, 2, \ldots, N_T/2$. It can be shown [16] that $z_i \equiv \mathrm{e}^{\gamma_i s}$ corresponds to one of the eigenvalues of $[Y_0]^{\dagger}[Y_1]$, where $[Y_0]^{\dagger}$ is the pseudo inverse of $[Y_0]$ and can be obtained by the well-known singular value decomposition (SVD) algorithm available in the IMSL library. The number of modes n can be determined from the number of singular values which are significantly larger than the noise level during the SVD analysis. Given the eigenvalue z_i and consequently, the propagation constant γ_i, the modal voltage c_i becomes readily available from (8) [19]. Without loss of generality, the mode indices $i = 1$ and 2 are chosen to denote the incoming and outgoing waves. Then, the incoming and outgoing modal amplitudes for even mode at port 2 can be found by $a_{2e} \equiv c_1/\sqrt{Z_e}$ and $b_{2e} \equiv c_2/\sqrt{Z_e}$. Here, Z_e is the characteristic impedance of the even mode, which is calculated *a priori* by 2-D spectral domain analysis [20].

The voltage of slotline (or odd) mode at the sampled points can be determined from the difference of the line voltages across the two slots. Following a similar procedure, the incoming and outgoing modal amplitudes for odd mode at port 2, a_{2o} and b_{2o} can be extracted. The whole process is repeated for port 1 to extract the desired modal amplitudes a_{1e}, b_{1e}, a_{1o}, and b_{1o}. These modal amplitudes can be related by a 4×4 scattering matrix, i.e.,

$$\begin{bmatrix} b_{1e} \\ b_{1o} \\ b_{2e} \\ b_{2o} \end{bmatrix} = \begin{bmatrix} \Gamma_{ee} & \Gamma_{eo} & T_{ee} & T_{eo} \\ \Gamma_{oe} & \Gamma_{oo} & T_{oe} & T_{oo} \\ T_{ee} & T_{eo} & \Gamma_{ee} & \Gamma_{eo} \\ T_{oe} & T_{oo} & \Gamma_{oe} & \Gamma_{oo} \end{bmatrix} \begin{bmatrix} a_{1e} \\ a_{1o} \\ a_{2e} \\ a_{2o} \end{bmatrix}. \tag{10}$$

For example, Γ_{oe} is the reflection coefficient of the odd mode due to an incident even mode of unit amplitude, and T_{ee} is the transmission coefficient of the even mode.

It deserves mentioning that there is no unanimous definition of the characteristic impedance due to the ambiguity of the current and voltage in non-TEM modes [21]. The scattering parameters between modes of the same characteristic impedance, say $\Gamma_{ee}, \Gamma_{oo}, T_{ee}$, and T_{oo}, is irrelevant to the definition of characteristic impedance. They can be determined from the corresponding modal voltage c_i's as well. And this is just the case discussed in [22]. However, the scattering parameters between even and odd modes will depend on how the characteristic impedances Z_e and Z_o are defined. Here, the voltage-power definition of characteristic impedance should be adopted. The definition can remove the ambiguity of the voltage due to the non-TEM nature of the guided modes and consequently, the magnitude square of the modal amplitude is the power carried by that mode, as required in the convention of the scattering matrix.

Due to the structure symmetry, the scattering matrix in (10) includes eight different elements, for which the same number of linear independent equations is required. The extracted modal amplitudes under one suitable excitation can be substituted into (10) to render four equations between the unknown scattering parameters. Choosing another independent excitation will suffice to solve the desired scattering matrix. In the numerical analysis, we simply choose the first excitation of $I_1 = 1$ and all others zero in Fig. 2. The equivalent magnetic current can be solved from (7). The matrix pencil approach is

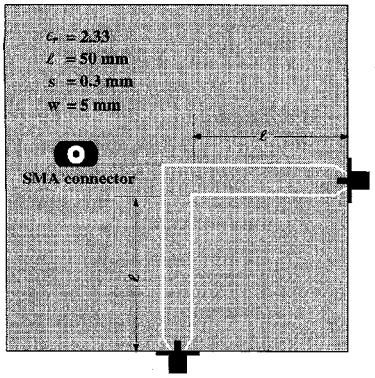

Fig. 4. The top view of the test fixture with SMA connectors. ($w = 0.5$ cm, $s = 0.03$ cm, $\ell = 5$ cm, $\epsilon_r = 2.33, h = 1.58$ mm). Figure is not drawn to scale.

then employed to extract all the modal amplitudes which are denoted by a_i^1 and b_i^1 ($i = 1e,\ 1o,\ 2e$, and $2o$). Similarly, another set of the modal amplitudes a_i^2 and b_i^2 are extracted by choosing the second excitation of $I_2 = 1$ and all others zero. Substitution of these two sets of modal amplitudes in (10) yields the following equations

$$\begin{bmatrix} a_{1e}^1 & a_{1o}^1 & a_{2e}^1 & a_{2o}^1 \\ a_{2e}^1 & a_{2o}^1 & a_{1e}^1 & a_{1o}^1 \\ a_{1e}^2 & a_{1o}^2 & a_{2e}^2 & a_{2o}^2 \\ a_{2e}^2 & a_{2o}^2 & a_{1e}^2 & a_{1o}^2 \end{bmatrix} \begin{bmatrix} \Gamma_{ee} \\ \Gamma_{eo} \\ T_{ee} \\ T_{eo} \end{bmatrix} = \begin{bmatrix} b_{1e}^1 \\ b_{2e}^1 \\ b_{1e}^2 \\ b_{2e}^2 \end{bmatrix}$$
$$\begin{bmatrix} a_{1o}^1 & a_{1e}^1 & a_{2o}^1 & a_{2e}^1 \\ a_{2o}^1 & a_{2e}^1 & a_{1o}^1 & a_{1e}^1 \\ a_{1o}^2 & a_{1e}^2 & a_{2o}^2 & a_{2e}^2 \\ a_{2o}^2 & a_{2e}^2 & a_{1o}^2 & a_{1e}^2 \end{bmatrix} \begin{bmatrix} \Gamma_{oo} \\ \Gamma_{oe} \\ T_{oo} \\ T_{oe} \end{bmatrix} = \begin{bmatrix} b_{1o}^1 \\ b_{2o}^1 \\ b_{1o}^2 \\ b_{2o}^2 \end{bmatrix}. \quad (11)$$

Now, all the elements of the scattering matrix can be determined accordingly. Note that the two ports are assumed to be the same in this study. In case of nonidentical ports, the above procedure can be applied as well except that four independent excitations will be required to determine the whole sixteen elements in the scattering matrix.

III. Experiments

Experiments are performed on a CPW line with a 90° bend to verify the accuracy of the theoretical results. As illustrated in Fig. 4, the test fixture is fabricated on a Duroid substrate ($\epsilon_r = 2.33$) of 1.58 mm thickness, and simply terminated with SMA connectors attached to an HP 8510B Network Analyzer. Since the connectors will block the propagation of the odd mode, only the even mode can be actually measured in the present setup. A thru-reflect-line (TRL) calibration is done to eliminate the connectors' effect for the even mode and to place the two reference planes shown in Fig. 1. Note that the calibration is successful only if the connectors are symmetrically soldered to the two sides of the CPW such that no coupling between the even and odd modes happens there.

Since it is unable to match the both modes at the ends, the present setup can not measure the elements of the 4×4 scattering matrix directly and separately. The connector which is nearly a short to the odd mode will reflect the back-propagating odd mode back to the input port of the discontinuity. Hence, the modal amplitudes of the incident and reflected waves for the odd mode at port 1 will satisfy

$$a_{1o} = -e^{-2\gamma_o d} b_{1o}; \qquad d = \ell + \Delta \quad (12)$$

and similarly at port 2. Here, ℓ is the length of the CPW section and Δ denotes the equivalent extension length of the connector for the odd mode. By a first order approximation, the extension length can be intuitively attributed to two factors, one is a quarter of the circumference of the connector's outer conductor and the other is an equivalent length corresponding to the inductance of short-end discontinuity.

By substituting (12) into (10) and equating the second and fourth rows, the modal amplitudes of the incident odd modes can be related to those of the incident even modes by

$$\begin{bmatrix} a_{1o} \\ a_{2o} \end{bmatrix} = -\begin{bmatrix} e^{2\gamma_o d}+\Gamma_{oo} & T_{oo} \\ T_{oo} & e^{2\gamma_o d}+\Gamma_{oo} \end{bmatrix}^{-1} \begin{bmatrix} \Gamma_{oe} & T_{oe} \\ T_{oe} & \Gamma_{oe} \end{bmatrix} \begin{bmatrix} a_{1e} \\ a_{2e} \end{bmatrix}. \quad (13)$$

Given the relations in (13), the first and third rows in (10) depict that the measured 2×2 scattering matrix for the even modes can be written as

$$\begin{bmatrix} S_{11} & S_{12} \\ S_{21} & S_{22} \end{bmatrix} = \begin{bmatrix} \Gamma_{ee} & T_{ee} \\ T_{ee} & \Gamma_{ee} \end{bmatrix} - \begin{bmatrix} \Gamma_{eo} & T_{eo} \\ T_{eo} & \Gamma_{eo} \end{bmatrix} \times \begin{bmatrix} e^{2\gamma_o d} + \Gamma_{oo} & T_{oo} \\ T_{oo} & e^{2\gamma_o d} + \Gamma_{oo} \end{bmatrix}^{-1} \begin{bmatrix} \Gamma_{oe} & T_{oe} \\ T_{oe} & \Gamma_{oe} \end{bmatrix}. \quad (14)$$

IV. Numerical Results and Discussion

The present theory is first applied to deal with the bend discontinuity whose dimensions are shown in Fig. 4. The moment method is applied to solve the equivalent magnetic current on the apertures. In numerical computation, the slot is divided into three cells along the width of the slot as shown in Fig. 3. The truncated length L of the CPW line is chosen to be about two guided wavelengths, which has been found sufficient to achieve convergent extracted modal amplitudes [19], [22]. In the meantime, the interval s of the division cell along the CPW line is chosen to be about one-fortieth wavelength, which is enough to represent the variations of the field satisfactorily. As a result, each slot is divided into about 90 cells along the longitudinal direction. The calculated slot voltage near the bend discontinuity and the truncated end includes significant contributions from the higher order modes, which will deteriorate the extraction for the desired guided modes. Hence, only the information on a center section of about 70 sampled data is actually employed in the matrix pencil method to extract the desired scattering parameters.

For the sake of comparison, a simpler division using only one cell along the width is also employed. The difference between the results by the two different divisions is not significant, which means that the simpler division is sufficient in this case. The main reason is that the slot width is narrow enough to neglect the transverse component of the magnetic current [5], [23]. For wider slots, a more detailed division

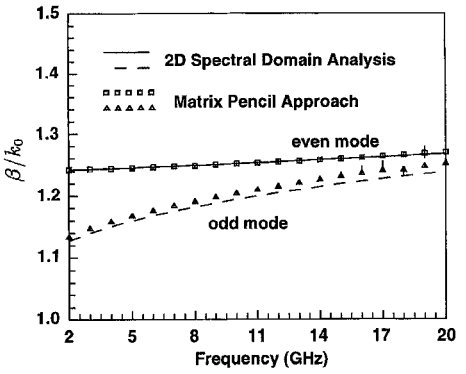

Fig. 5. The dispersion curves of the even and odd modes in the associated coplanar waveguide. Both the results extracted by the matrix pencil approach and those calculated by the 2-D spectral domain analysis are included for comparison.

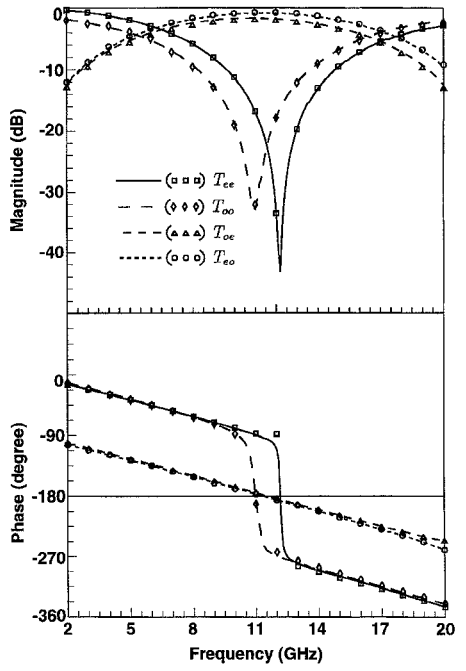

Fig. 6. The transmission coefficients of the bend discontinuity shown in Fig. 4. (The results denoted by continuous lines are obtained by assuming a uniform longitudinal magnetic current along the slot of CPW, while those marked with symbols are calculated by employing a more detailed division of three cells along the slot width.)

will be necessary to include the longitudinal component and model the nonuniform field distribution in the transverse direction.

Given the magnetic current distribution, the matrix pencil approach is employed to extract the propagation constants and modal amplitudes of all the guided modes. Fig. 5 shows the calculated propagation constants versus the frequency for both the even and odd modes. Note that the matrix pencil method should be employed four times to extract all the modal amplitudes in (11) at each frequency. The extracted propagation constants for the same mode are found to be not exactly the same. The results in the figure are thus marked with bars of finite sizes to denote the range over which the numerical values distribute. The size of the bar somewhat

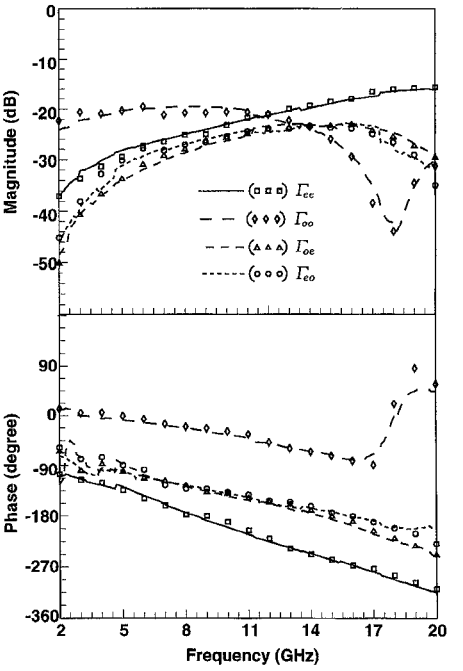

Fig. 7. The reflection coefficients of the bend discontinuity shown in Fig. 4.

depicts the computation error, part of which may be attributed to the insufficient length of the line sections. Numerical experiments validate that increasing the length of line sections can reduce the high frequency discrepancy. For the sake of comparison, the well-known 2-D spectral domain analysis [20] is also applied to calculate the propagation constants, which are denoted by the solid and dashed curves. Reasonable agreement can be found between the results by these two methods.

The full 4×4 scattering matrix which characterizes the bend discontinuity can be obtained from the extracted modal amplitudes by using (11). Fig. 6 shows the magnitude and phase of all the transmission coefficients between both the even and odd modes. The transmission coefficients between different modes, T_{eo} and T_{oe}, signify the occurrence of the mode conversion. It is noted from the figure that T_{oe} and T_{eo} reach the maximum while T_{oo} and T_{ee} become very small in a certain frequency range. It means that one mode converts almost completely to the other after passing through the bend. This is expected, since the path difference between the outer and inner slots is close to a half of waveguide wavelength. Consequently, it becomes a challenge to preserve good transmission through the CPW bend for the even mode in this frequency range. Using the air bridge can suppress the occurrence of the odd mode, but will in the same time increases dramatically the reflection coefficient as depicted in (14). Of course, it will not work well either to miter the corner as in the microstrip line [24]. However, from another point of view, the mode conversion phenomenon offers a promising way in the design of CPW to coupled slotline transition.

The magnitude and phase of the reflection coefficients are shown in Fig. 7. In general, the reflection coefficients are one order of magnitude smaller than the transmission coefficients. They are comparatively more sensitive to numerical errors

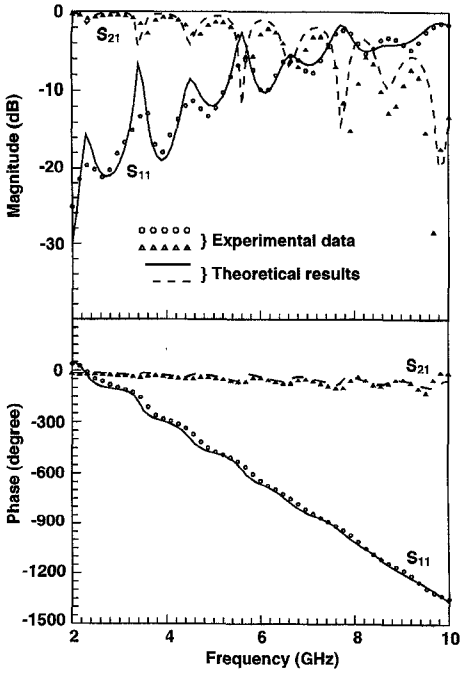

(a)

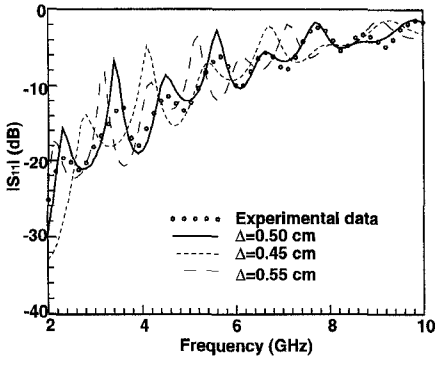

(b)

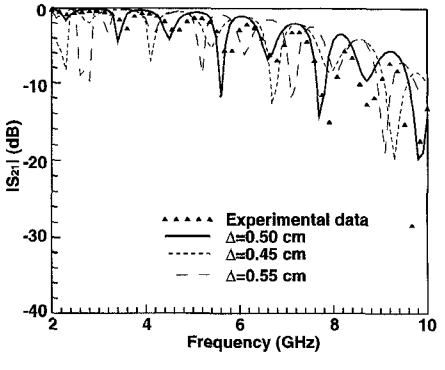

(c)

Fig. 8. Comparison between the measured S-parameters of the coplanar waveguide bend shown in Fig. 4 and the theoretical prediction but with different trial extension length Δ as a parameter. (a) Magnitude and phase of S_{11} and S_{21}, (b) magnitude of S_{11}, and (c) magnitude of S_{21}.

and therefore show undesirable ripples in the figure. It is worth mentioning that the reciprocity theory is not explicitly imposed in the determination of the scattering matrix by (11). As a result, the calculated results for the mode conversion coefficients Γ_{eo} and Γ_{oe} (and similarly for T_{eo} and T_{oe} in Fig. 6) are slightly different. The discrepancy is quite small at low frequencies but may become as large as 15% at higher frequencies, where the mode conversion is less significant and therefore susceptible to numerical errors.

Fig. 8 shows the measured S-parameters of the CPW bend of Fig. 4 in the range of 2 to 10 GHz. The solid and dashed curves denote the theoretical results which are obtained from the extracted 4×4 scattering matrix by (14). The extension length Δ is chosen as 0.5 cm, which is found to yield good agreement in the slope of the phase of the reflection coefficient. The adjustment is necessary since the effect of the connectors is unavailable and it influences the results seriously. Other extension lengths, say $\Delta = 0.45$ cm and 0.55 cm, have been tried and the results are plotted in the same figure to depict the sensitivity of theoretical S_{11} and S_{21} to the values of Δ. They fail to predict reasonably the ripples in the measured $|S_{11}|$ and $|S_{21}|$. The ripples in Fig. 8 signify the strong interaction between the even and odd modes, and therefore the phase difference between the two modes is important. The agreement between the theoretical results with suitable chosen Δ and the experimental data is very good in the lower frequency range, which validates the accuracy of the present algorithm. The deviation in the higher frequency range can be partly attributed to the unpredictable high frequency characteristics of the connectors.

V. Conclusion

A CPW 90° bend has been analyzed successfully by combining the MPIE formulation, the moment method, and the matrix pencil approach. The algorithm can be generalized to deal with other CPW discontinuities consisting of several input ports. The number of guided modes in each port can be arbitrary and furthermore, the propagation constant of each guided mode need not be known *a priori*.

Theoretical results for the full 4×4 scattering matrix of the bend discontinuity have been presented and verified indirectly by the experiment. The mode conversion phenomenon has been for the first time characterized thoroughly. The phenomenon becomes very significant when the path difference between the outer and inner slots of the bend is close to a half of waveguide wavelength. In this frequency range, it is very difficult to suppress the occurrence of the odd mode while keeping a small reflection coefficients of the even mode. However, from another point of view, this significant mode conversion may find applications in the design of CPW to coupled slotline transition.

References

[1] C. P. Wen, "Coplanar waveguide: A surface strip transmission line suitable for nonreciprocal gyromagnetic device applications," *IEEE Trans. Microwave Theory Tech.*, vol. MTT-17, pp. 1087–1090, Dec. 1969.

[2] R. W. Jackson, "Considerations in the use of coplanar waveguide for millimeter-wave integrated circuits," *IEEE Trans. Microwave Theory Tech.*, vol. MTT-34, pp. 1450–1456, Dec. 1986.

[3] T. Hirota, Y. Tarusawa, and H. Ogawa, "Uniplanar MMIC hybrids–a proposed new MMIC structure," *IEEE Trans. Microwave Theory Tech.*, vol. MTT-35, pp. 576–581, June 1987.

[4] M. Riaziat, I. Zubeck, S. Bandy, and G. Zdasiuk, "Coplanar waveguides used in 2-18GHz distributed amplifier," in *1986 IEEE MTT-S Int. Microwave Symp. Dig.*, pp. 337–338.
[5] A. A. Omar and Y. L. Chow, "Coplanar waveguide with top and bottom shields in place of air bridges," *IEEE Trans. Microwave Theory Tech.*, vol. MTT-41, pp. 1559–1563, Sept. 1993.
[6] N. I. Dib, P. B. Katehi, and G. Ponchak, "Analysis of shielded CPW discontinuities with air-bridges," in *1991 IEEE MTT-S Int. Microwave Symp. Dig.*, pp. 469–472.
[7] R. Bromme and R. H. Jansen, "Systematic investigation of coplanar waveguide MIC/MMIC structures using a unified strip/slot 3D electromagnetic simulator," in *1991 IEEE MTT-S Int. Microwave Symp. Dig.*, pp. 1081–1084.
[8] M. Rittweger, M. Abdo, and I. Wolff, "Full-wave analysis of coplanar discontinuities considering three-dimensional bond wires," in *1991 IEEE MTT-S Int. Microwave Symp. Dig.*, pp. 465–468.
[9] A. A. Omar and Y. L. Chow, "A solution of waveguide with air-bridges using complex images," *IEEE Trans. Microwave Theory Tech.*, vol. MTT-40, pp. 2070–2077, Nov. 1992.
[10] T. Becks and I. Wolff, "Full-wave analysis of various coplanar bends and T-junctions with respect to different types of air-bridges," *1993 IEEE MTT-S Int. Microwave Symp. Dig.*, pp. 697–700.
[11] N. I. Dib, G. Ponchak, and P. B. Katehi, "A theoretical and experimental study of coplanar waveguide shunt stubs," *IEEE Trans. Microwave Theory Tech.*, vol. MTT-41, pp. 38–44, Jan. 1993.
[12] N. I. Dib, M. Gupta, G. E. Ponchak, and L. P. B. Katehi, "Characterization of asymmetric coplanar waveguide discontinuities," *IEEE Trans. Microwave Theory Tech.*, vol. MTT-41, pp. 1549–1558, Sept. 1993.
[13] N. H. Koster, S. Koblowski, R. Bertenburg, S. Heinen, and I. Wolff, "Investigation of air bridges used for MMIC's in CPW technique," in *Proc. 19th European Microwave Conf.*, Sept. 1989, pp. 666–671.
[14] R. F. Harrington, *Time-Harmonic Electromagnetic Fields.* New York: McGraw-Hill, 1961, ch. 2.
[15] R. F. Harrington, *Field Computations by Moment Methods.* New York: Macmillan, 1968, ch. 1.
[16] Y. Hua and T. K. Sarkar, "Generalized pencil-of-function method for extracting poles of an EM system from its transient response," *IEEE Trans. Antennas Propagat.*, vol. AP-37, pp. 229–234, Feb. 1989.
[17] J. R. Mosig, "Integral equation technique," T. Itoh, Ed., in *Numerical Techniques for Microwave and Millimeter-Wave Passive Structures.* New York: Wiley, 1989, pp. 133–207.
[18] M. Drissi, V. F. Hanna, and J. Citerne, "Analysis of coplanar waveguide radiating end effects using the integral equation technique," *IEEE Trans. Microwave Theory Tech.*, vol. 39, pp. 112–116, Jan. 1991.
[19] S. G. Hsu and R. B. Wu, "Full wave characterization of a through hole via using the matrix-penciled moment method," *IEEE Trans. Microwave Theory Tech.*, vol. 42, pp. 1540–1547, Aug. 1994.
[20] T. Uwaro and T. Itoh, "Spectral domain approach," T. Itoh, Ed., in *Numerical Techniques for Microwave and Millimeter-Wave Passive Structures.* New York: Wiley, 1989, pp. 334-380.
[21] B. Bianco, L. Panini, M. Parodi, and S. Ridella, "Some considerations about the frequency dependence of the characteristic impedance of uniform microstrips," *IEEE Trans. Microwave Theory Tech.*, vol. MTT-26, pp. 182–185, Mar. 1978.
[22] T. K. Sarkar, Z. A. Maricevic, and M. Kahrizi, "An accurate de-embedding procedure for characterizing discontinuities," *Int. J. Microwave and MM-wave Computer Aided Eng.*, vol. 2, no. 3, pp. 135–143, 1992.
[23] N. I. Dib, L. P. B. Katehi, G. E. Ponchak, and R. N. Simons, "Theoretical and experimental characterization of coplanar waveguide discontinuities for filter applications," *IEEE Trans. Microwave Theory Tech.*, vol. 39, pp. 873–881, May 1991.
[24] R. J. P. Douville and D. S. James, "Experimental study of symmetric microstrip bends and their compensation," *IEEE Trans. Microwave Theory Tech.*, vol. MTT-26, pp. 175–182, Mar. 1978.

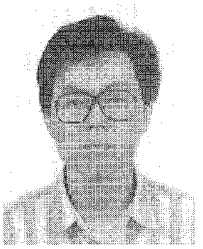

Ming-Dong Wu was born in Taipei, Taiwan, Republic of China, in 1967. He received the B.S. degree in electrical engineering from Tatung Institute of Technology, Taipei, Taiwan, in 1989, and the M.S. and Ph.D. degrees in electrical engineering from National Taiwan University, Taipei, Taiwan in 1991 and 1995, respectively.

His research interests include the transmission line discontinuities and microstrip antennas.

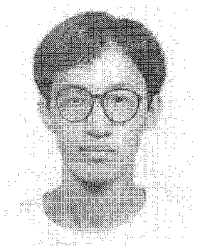

Sheng-Ming Deng was born in Taidon, Taiwan, Republic of China, in 1965. He received the B.S. degree in electrical engineering from National Cheng-Kung University, Tainan, Taiwan, in 1988, and the M.S. and Ph.D. degrees in electrical engineering from National Taiwan University, Taipei, Taiwan in 1990 and 1995, respectively.

His research interests include the analysis and design of microstrip antennas and microwave circuits.

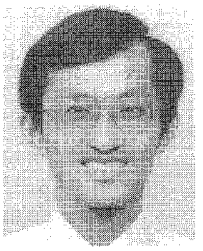

Ruey-Beei Wu was born in Tainan, Taiwan, Republic of China, in 1957. He received the B.S.E.E. and Ph.D. degrees from National Taiwan University, Taipei, Taiwan, in 1979 and 1985, respectively.

In 1982, he joined the faculty of the Department of Electrical Engineering, National Taiwan University, where he is now a Professor. From 1986 to 1987, he was a Visiting Scientist in IBM General Technology Division Laboratory, East Fishkill Facility, Hopewell Junction, NY. His current research interests include computational electromagnetics, dielectric waveguides, slot antennas, transmission line discontinuities, and interconnection modeling for computer packaging.

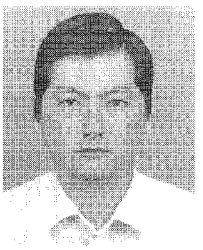

Powen Hsu was born in Taipei, Taiwan, Republic of China, in 1950. He received the B.S. degree in physics from National Tsing-Hua University, Hsinchu, Taiwan, in 1972, the M.S. degree in physics from the University of Maryland, College Park, in 1976, and the M.S. and Ph.D. degrees in electrical engineering from the University of Southern California, Los Angeles, in 1978 and 1982, respectively.

From 1982 to 1984, he was with ITT Gilfillan, Van Nuys, CA, where he engaged in research and development pertaining to radar antenna systems. In 1984 he joined the faculty of National Taiwan University, Taipei, Taiwan, where he is currently a Professor of Electrical Engineering Department and was Department Chairperson from 1992 to 1995. His current research interests include the design and analysis of waveguide slot arrays, microstrip antennas, and microwave and millimeter-wave integrated circuits.